Biocatalysis and Agricultural Biotechnology 18 (2019) 101069

Contents lists available at ScienceDirect

Biocatalysis and Agricultural Biotechnology

journal homepage: www.elsevier.com/locate/bab

An investigation of antibiofilm and cytotoxic property of MgO nanoparticles

D. MubarakAli[a,b,c,*], Muhammed A.P. Manzoor[d,1], A. Sabarinathan[b], C. Anchana Devi[e], P.D. Rekha[d], N. Thajuddin[b], Sang-Yul Lee[c,**]

[a] School of Life Sciences, B.S. Abdur Rahman Crescent Institute of Science and Technology, Chennai, 600048, India
[b] National Repository for Microalgae and Cyanobacteria – Freshwater (DBT, Govt. of India), Department of Microbiology, Bharathidasan University, Tiruchirappalli, 620024, Tamil Nadu, India
[c] Centre for Surface Technology and Applications (CeSTA), Department of Materials Engineering, Korea Aerospace University, Republic of Korea
[d] Yenepoya Research Centre, Yenepoya University, Mangalore, 575018, Karnataka, India
[e] PG Research Department of Biotechnology, Women's Christian College, Chennai, India

ARTICLE INFO

Keywords:
MgO nanoparticles
Anti-biofilm
MCF-7
Cytotoxicity
Apoptosis
Uropathogenic bacteria

ABSTRACT

MgO nanoparticles (MgONPs) have been widely used as antibacterial agents with the advantages of them being nontoxic and their unique biological properties. In this study, we synthesized MgONPs by co-precipitation method and characterized them by XRD, SEM and EDS analysis. The antibiofilm activity of MgONPs as observed quantitatively by crystal violet assay and their action on biofilm architecture were assessed in both Gram-positive and Gram negative uropathogenic bacteria. In addition, the cytotoxic effect of synthesized MgONPs was evaluated against human breast cancer, MCF-7 cells. The morphological changes of apoptosis were observed by Acridine Orange/Ethidium Bromide (AO/EB) staining using a fluorescent microscope. MgONPs inhibited more than 50% of the biofilms in most of the tested uropathogenic bacteria; notably 80% inhibition in the case of *K. pneumoniae*. MgONPs successfully inhibited the viability of MCF-7 cells at a concentration of 50 $\mu g.mL^{-1}$. Given their antibiofilm properties; MgONPs could be used as a potential nanomaterial for *in vivo* applications such as coating for a medical implant.

1. Introduction

Nanotechnology is an area of emerging interest in the field of science and technology due to its wide variety of applications in the field of biomedicine, optics, and electronics; especially for purpose of developing new nanoscale materials (Albrecht et al., 2006). Various physical, chemical, biological, and hybrid methods are currently being employed for nanoparticle synthesis (MubarakAli et al., 2015a,b). Nanoparticles can be made by using various biological substrates such as bacteria, algae, diatom, actinomycetes, plants, and biomolecules (Priyadarshini et al., 2013; MubarakAli et al., 2011a, 2011b; MubarakAli et al., 2011a,b,c, 2013a,b).

Urolithiasis (kidney stone disease) is one of the most common urological diseases with high prevalence globally (Manzoor et al., 2017 and 2018a). Urinary tract infections (UTIs) and urolithiasis are inevitably linked and studies suggested that patients with kidney stone are more likely to have UTIs than the normal population (Barr-Beare et al., 2015). Bacterial biofilms play an important role in urolithiasis and many bacteria causing UTIs are associated with biofilm formation (Shabeena et al., 2018, Manzoor et al., 2018b, 2018c, 2018d). The biofilms are multi-cellular, surface-attached microbial communities with particular physiologic and architecture characteristics, which can sometimes confer resistance to different classes of antibiotics (Vahedi et al., 2017). This biofilm formation is an important virulence factor for a wide range of microbes that cause chronic infections, and are responsible for 75% of human microbial infections (Koo et al., 2017). Most of the Gram positive and Gram negative bacteria have the ability to form biofilms and main ones include *Escherichia coli, Klebsiella pneumoniae, Enterococcus faecalis, Staphylococcus aureus, Streptococcus viridans, Proteus mirabilis* and *Pseudomonas aeruginosa* (Donlan, 2001; MubarakAli et al., 2015).

The control of the bacterial biofilm formation is of importance for public health and economy, especially in the case nosocomial infections which leads to various life-threatening diseases (Naiyf, and Jamal, 2017). Several synthesized nanoparticles have shown their effectiveness for treating infectious microbes, including antibiotic-resistant

* Corresponding author. School of Life Sciences, B.S. Abdur Rahman Crescent Institute of Science and Technology, Chennai, 600048, India.
** Corresponding author.
E-mail addresses: mubarakali.sls@crescent.education, mubinano@gmail.com (D. MubarakAli), sylee@kau.ac.kr (S.-Y. Lee).
[1] Present Address: ICAR–Indian Institute of Spices Research, Kozhikode, 673012, Kerala, India.

https://doi.org/10.1016/j.bcab.2019.101069
Received 17 November 2018; Received in revised form 19 February 2019; Accepted 27 February 2019
Available online 04 March 2019
1878-8181/

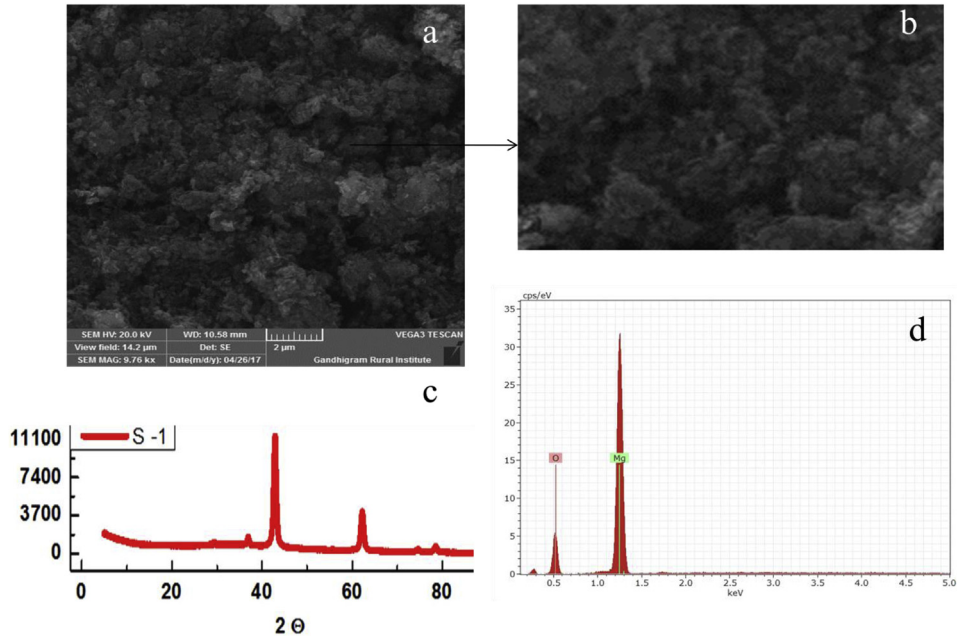

Fig. 1. Investigation of MgONPs: fine spherical shaped nanoparticles in slightly agglomerated form (a,b); sharp plane at the 42 °C (c) elemental signals, Mg and O at a high percentage (d).

strains (Huh et al., 2011; Ghosh et al., 2015). Several studies have demonstrated the *in vitro* inhibition of bacterial biofilm by various nanoparticles (Markowska et al., 2013). Most of the nanoparticles such as silver, gold, copper, and zinc have the ability to inhibit the biofilm growth (Gopinath et al., 2015; Chari et al., 2017; LewisOscar et al., 2015). Furthermore, certain inorganic nanoparticles have important implications for the treatment of microbial infections and post-surgical complication as wound dressing materials (Gopinath et al., 2012; MubarakAli et al., 2013a,b). Breast cancer is one of the most common cancers worldwide. The global burden of breast cancer exceeds all other cancers and it is a leading cause of cancer death in women and the incidence rates of breast cancer are increasing globally (Jemal et al., 2010). One of the main advantages of these nanoparticles is their low cytotoxicity and antioxidant property (MubarakAli et al., 2018). Importantly, some of the synthesized nanoparticles have been shown to be effective against a broad range of human breast cancer cells (Jeyaraj et al., 2013). MCF-7 is a widely used epithelial cancer cell line, derived from breast adenocarcinoma and used for *in vitro* breast cancer studies (Lee et al., 2015).

Magnesium oxide (MgO) is a versatile biomaterial, with wide applications in materials science and biomedical diagnostics. However, the toxicity of nanoparticles of MgO to bacterial/human cells and organs remains fairly unknown. The role of MgONPs as efficient biofilm inhibitors has not yet been given considerable attention (Hayat et al., 2018). Therefore, the present study was designed to synthesize and characterize MgONPs, and the antibiofilm potential was assessed against urolithiasis associated uropathogenic bacteria. The MgONPs were characterized using X-ray diffraction (XRD), fourier transform infrared (FTIR) spectscopy, scanning electron microscopy (SEM) and energy dispersive spectroscopy (EDS). The biofilm architecture was analyzed by CLSM. In addition, the anti-cancer activity was studied using MCF-7 breast cancer cell line and the relative rate of proliferation was studied by Acridine Orange/Ethidium Bromide (AO/EB) apoptotic staining method using a fluorescent microscope.

2. Materials and methods

2.1. Materials

Chemicals such as Acridine orange ($C_{17}H_{19}N_3$), ethidium bromide ($C_{21}H_{20}BrN_3$), 3-(4,5-dimethyl-2-thiazolyl)-2,5-diphenyl-2H-tetrazolium bromide (MTT) (RM1131, Hi-media Mumbai), and Dimethyl sulfoxide (DMSO) were purchased from Sigma Aldrich (St Louis, MO, USA).

2.2. Collection of clinical samples, cell culture, and maintenance

Ten clinical strains of bacteria including Gram positive and Gram negative strains were obtained from the Yenepoya Research Centre in Mangalore, India and sub-cultured on Luria Bertani Agar. The morphological and physiological characterization of the clinical isolates was performed according to the methods described in Bergey's Manual of Determinative Bacteriology (Buchanan and Gibbons, 1974). The 16S rDNA sequencing was performed earlier for the identification of the bacteria as described earlier (Chandra et al., 2017). Human breast cancer cell line (MCF-7) was obtained from National Centre for Cell Science (NCCS), Pune. The cells were maintained in Dulbecco's Modified Eagle's Medium (DMEM) supplemented with 10% fetal bovine serum (FBS) and 1% antibiotic (penicillin 10000 U/mL, 10 mg streptomycin and 25 µg amphotericin B per ml in 0.9% normal saline). The cells were maintained in 5% CO_2 humidified incubator at 37 °C. During subculture, the cells were detached from the flask by trypsinization when they reached 80% confluency and splited using DMEM (1:4).

2.3. Synthesis and characterization of MgONPs

Briefly, MgONPs were synthesized with an optimized concentration of magnesium nitrate hexahydrate (0.1 M) and NaOH (0.5 M) dissolved in 200 mL of distilled water. Then, 200 mL of NaOH solution was added to the solution of ($Mg(NO_3)_2{\cdot}6H_2O$) drop-wise. The solution was kept under magnetic stirrer for 2 hr and after stirring the solution was kept for 2 hr. The precipitate was filtered and washed several times using distilled water and ethanol. The final product was kept in a hot air oven (Ausco, Chennai) at 80 °C for drying and removes moisture. The dried

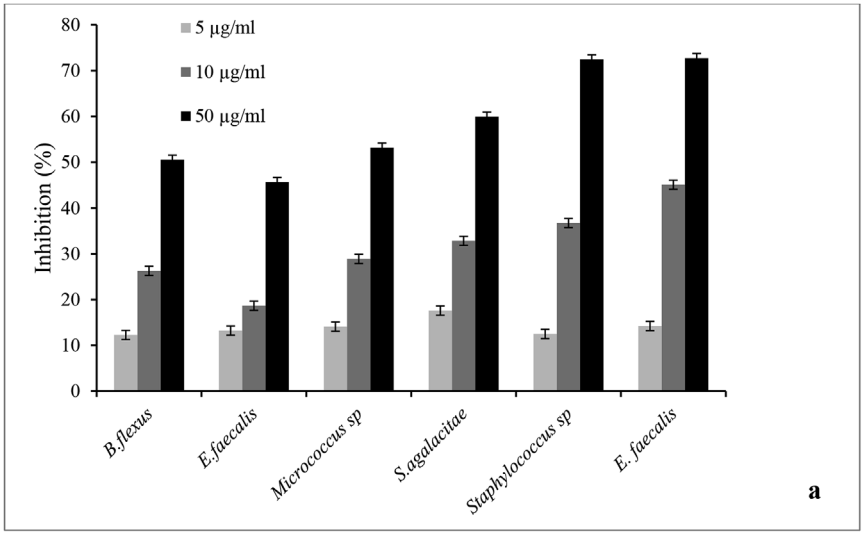

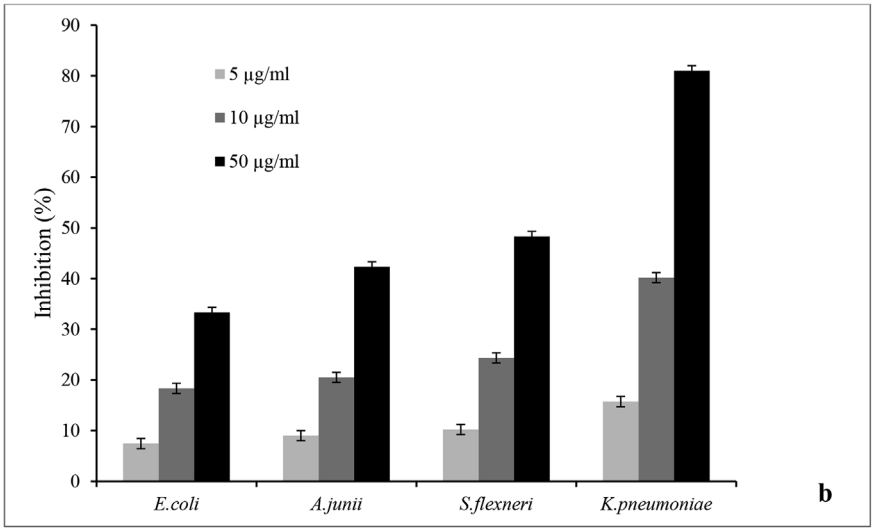

Fig. 2. Antibiofilm activity of MgONPs against Gram-positive (a) and Gram-negative (b) uropathognic bacteria.

powders were ground to fine powder using a mortar pestle. The nanoparticles were treated at high temperature with the limited supply of air or oxygen (calcination). The calcination temperature will active the specific surface area of the nanocatalyst to improve their efficiency for their process. The final product of MgO was calcined in a muffle furnace (Indfurr, India) which was operated at 230 volts, 1 phase, and 50 Hz, AC and the fine powder of MgO was calcinated at 400 °C for 4 hr for the removal of impurities present in the powder. The dried powder was examined using XRD and SEM with EDS for the investigation of the shape and size of the nanoparticles (Manzoor et al., 2019).

2.4. Biofilm formation assay

Biofilm formation was quantified using the method reported elsewhere with some modifications (Limsuwan and Voravuthikunchai, 2008). Overnight grown cultures of clinical isolates were diluted with fresh LB broth (1:20) with and without sub-inhibitory concentrations of MgO NPs (5–50 µg.mL^{-1}). This suspension (200 µL) was dispensed into 96-well microtiter plate (Thermo Scientific, USA) and incubated at 37 °C for 24 hr. After incubation, the planktonic cells were discarded and the well was thoroughly rinsed twice with distilled water. Biofilms were quantified by staining the attached cells with 0.4% crystal violet for 30 min. The wells were washed thoroughly with saline in order to remove the excess dye, while crystal violet attached cells were solubilized in 250 µL of absolute ethanol and the absorbance was determined at 570 nm using microtiter plate reader (FLUOstar Omega). The percent of biofilm inhibition was determined using equation (1) (Chari et al., 2017).

$$\text{Biofilm inhibition (\%)} = ([\text{Abs}_{\text{Control}} - \text{Abs}_{\text{Test}}]/\text{Abs}_{\text{Control}}) \times 100 \quad (1)$$

The qualitative analysis of the control of clinical bacterial strains and MgONPs treated biofilms were performed using CLSM as described earlier (LewisOscar et al., 2015; Khan et al., 2019). Briefly, the bacterial biofilms were allowed to grow on glass pieces (1 × 1 cm) placed in 24-well polystyrene plates (Greiner Bio-One), supplemented with and without MgONPs and incubated for 24 hr at 37 °C. The biofilms were monitored under a CLSM (Carl Zeiss, Germany) after washing with PBS and staining with 0.01% acridine orange for 5 min. The 488 Ar laser and a 500–640 nm band emission filter were used to excite and detect the stained cells. Obtained images were analyzed for the surface area covered and biofilm thickness using the attached software (Carl Zeiss, Germany).

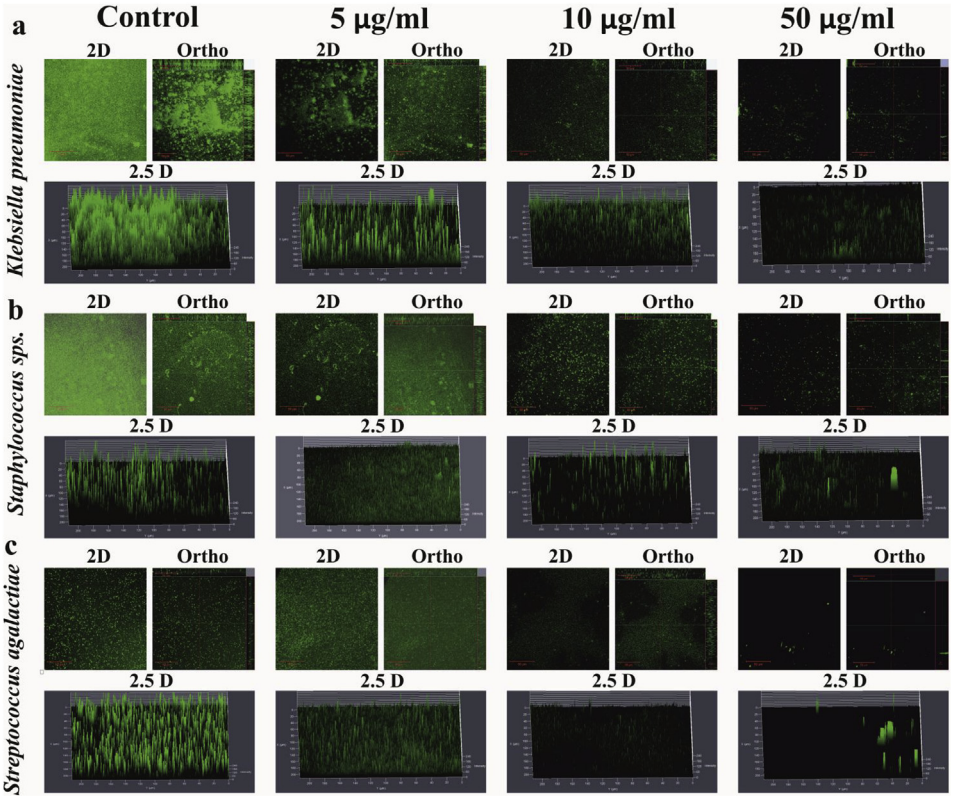

Fig. 3. CLSM micrographs of representative uropathogenic bacteria treated with and without MgONPs (a) *Klebsiella pneumoniae* (highly adherent strain) (b) *Staphylococcus* sps (moderately adherent strain) and (c) *Streptococcus agalactiae* (weakly adherent strain).

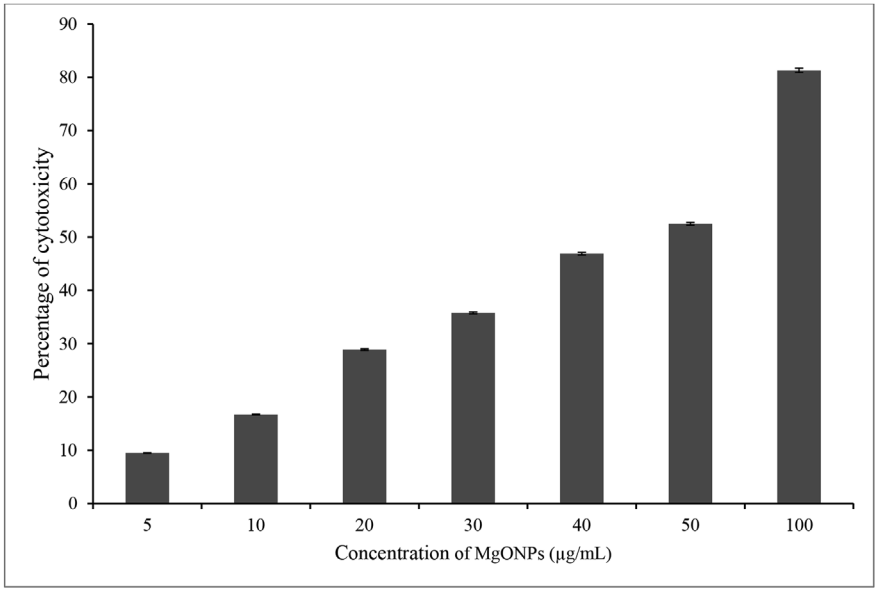

Fig. 4. Cytotoxicity of MgONPs against MCF-7 cells showing 50% of the reduction at the concentration of 50 $\mu g.mL^{-1}$.

2.5. Anticancer activity of MgONPs against MCF-7 cell lines

2.5.1. Cell viability assay

The relative rate of proliferation of MgONPs on MCF-7 breast cancer cells was determined using MTT colorimetric technique (Mosmann, 1983). The MgONPs were first weighed, and the required nanoparticles solution was prepared in sterile double-distilled water and diluted to the required concentrations (5, 10, 20, 30, 40, 50, and 100 $\mu g.mL^{-1}$) using the cell culture medium. The required concentrations of MgONPs were then added to the cell cultures to obtain the final concentration of MgONPs and incubated for 24 h in 5% CO_2 humidified incubator at 37 °C. Cells treated without the nanoparticles were used as controls. After 24 h of incubation, the cells were washed with PBS, and then 100 µL of the MTT reagent was added to each microtiter well. Microtiter plates were incubated for 4 h at 37 °C for the reduction of the MTT dye by normal living cells. Then, 100 µL of DMSO was added to each well to solubilize the Formazan crystals and the plates were kept in a dark for 15 min. The relative rate of proliferation on MCF-7 cells was detected

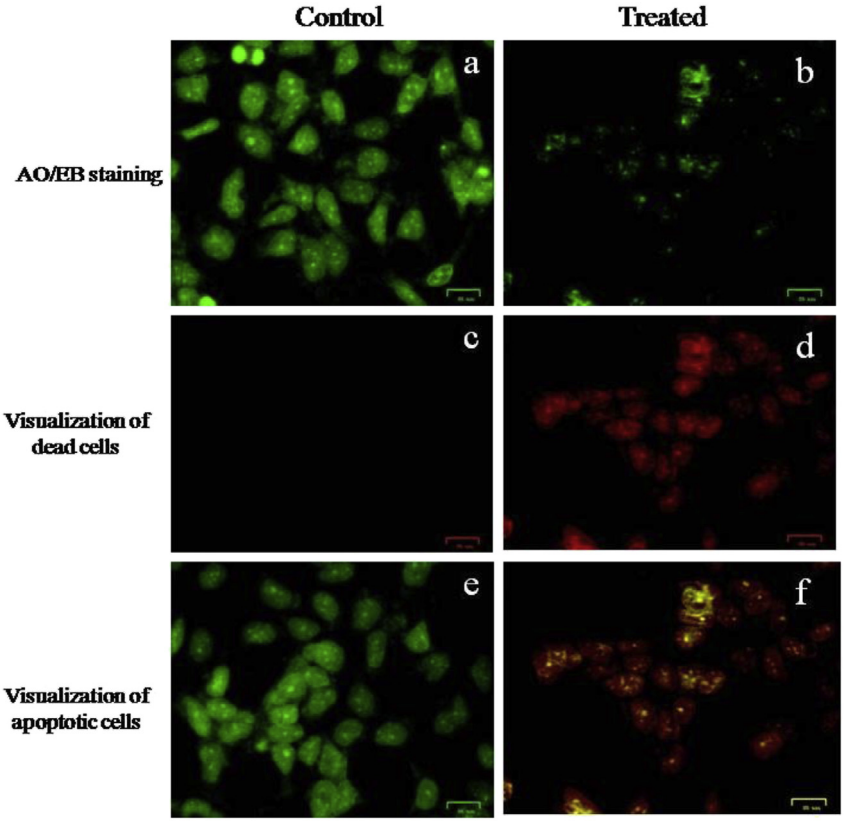

Fig. 5. Apoptotic effects of fluorescence microscopy study of AO/EB stain (a, b) Respective control (left) and treated (right) with MgONPs. (c–f) Cells stained green represent viable cells, whereas yellow staining represents early apoptotic cells and reddish or orange staining represents late apoptotic cells.

by eluting the dye with DMSO, and the optical density was measured using spectrophotometer (OD_{595} nm). The percentage of cell viability was calculated using equation (2). All experiments were performed in triplicates.

$$\text{Cell viability (\%)} = \text{Abs}_{\text{Sample}}/\text{Abs}_{\text{Control}} \text{ x } 100 \quad (2)$$

2.5.2. Morphological analysis of apoptosis by AO/EB dual staining

Acridine orange (AO) and ethidium bromide (EB) dual staining was used to detect the morphological evidence of apoptosis in the MgONPs treated cells (Darzynkiewicz and Li, 1994). The cells were fixed, washed with methanol and incubated 1 hr at room temperature. The cells were labeled with 1:1 ratio of AO and EB in PBS and incubated for 10 min then the excess unbind dye was removed by washing with PBS. Stained cells were visualized under a fluorescence microscope.

3. Results and discussion

The SEM, XRD and EDS pattern of MgONPs obtained from coprecipitation synthesis were as shown in Fig. 1(a–d). The synthesized MgONPs showed sharp plane showing at 42 °C by XRD analysis. A cluster of fine spherical nanoparticles was observed with the size range from 100 to 200 nm by SEM analysis. EDS spectrum showed Mg and O elemental signals at a high percentage. The antibiofilm efficacy of the MgONPs was evaluated against both Gram-positive and Gram-negative uropathogenic bacteria. Biofilm production was reported in all the strains. A standard crystal violet assay for biofilm biomass indicated that MgONPs were more effective in the eradication of preformed biofilm produced by all tested isolates (Fig. 2). Recent reports also suggested that MgONPs is a potential antibacterial agent against bacteria (Cai et al., 2018). The severely adherent strain was found as *K. pneumoniae* which showed 80.98% biofilm inhibition when treated with 10 $\mu g.mL^{-1}$ of MgONPs. In the case of *E. coli*, the obtained results revealed that only 33.33% of biofilm was inhibited when treated MgONPs which was the weakly adherent strain among tested isolates. Moderate activity was observed with the remaining microbial strains [*B. flexus* (50.25%), *Micrococcus sps* (54.65%), *S. agalacitae* (69.76%) and *Staphylococcus* sp. (74.3%)].

Visualization of bacterial biofilms with CLSM (2D, 2.5D, and Ortho and stacked images) showed a wide spectrum of morphological differences in biofilm architectures. The results clearly revealed a visible reduction of the biofilm in the treated samples (Fig. 3). The thickness of the biofilm was reduced and the morphological changes were clearly visible in the presence of MgONPs. Notably, large scattered cell aggregates were observed in the biofilms of *K. pneumonia* and there were less viable cells in the aggregates after 24 h exposure to the MgONPs (Fig. 3). When compared to control; the mat like the architecture of the MgO treated biofilm was reduced to individual cells.

This study investigated the inhibition of biofilm activity by synthesized MgONPs. Synthesized MgONPs were tested for biofilm inhibition potential against 10 different strains of uropathogenic bacteria. The antibiofilm activity of clinical isolates of Gram positive and Gram negative uropathogenic bacteria was clearly evident under *in vitro* conditions, subsequently leading the inhibition of biofilm formations. It was noticed that when the concentration of the MgONPs was increased, the inhibition of biofilm was also enhanced which can be attributed directly to the dose-dependent activity. We found a difference in the inhibitory pattern among the isolates and this highlights the application of these MgONPs as biofilm-disrupting agents against uropathogenic bacteria. The inhibitory activities of MgONPs as an effective therapeutic agent against various pathogens have been reported earlier (Huang et al., 2005; Leung et al., 2014). The inhibitory activities of MgONPs may be due to the efficacy of antimicrobial activity, physical properties like size, electrostatic interactions with bacterial envelope and other

chemical properties like affinity between the materials and the biofilm formation (Park et al., 2013; Zhang et al., 2012).

An MTT assay was performed to determine the anti-proliferative effect of MgONPs against MCF-7 breast cancer cells. MCF-7 cells were incubated with different concentration of MgONPs for 24 h. The results showed that MgONPs induced dose-dependent cytotoxic effects against MCF-7 cell line. On other hands, the relative rate of proliferation on MCF-7 cell lines increased with increasing concentration of MgONPs (Fig. 4). There was a change in the percentage of cell viability in control and MgONPs (5, 10, 50, 50, 100 $\mu g.mL^{-1}$) treated MCF-7 cells. The Inhibitory Concentration (IC_{50}) value associated with MgONPs was found to be 50 $\mu g.mL^{-1}$.

Apoptosis was examined using nuclear morphology by AO/EB staining. The results of the relative rate of proliferation were consistent with the observations from AO/EB staining. As shown in Fig. 5, control MCF-7 cells were stained with uniform green fluorescence and no apoptotic features were observed. Following treatment of MCF-7 cells with MgONPs for 24 h; obvious morphological changes and apoptotic cells were observed (Fig. 5). The results suggest that MgONPs induced MCF-7 cell apoptosis. Despite the progression of early diagnosis and treatment, it is imperative to discover alternative therapies, tools, and drugs to conquer the situation (Boca et al., 2011). Cytotoxicity is considered as a good anti-cancer parameter if it induces apoptotic pathways inside the cell. The IC_{50} of the MgONPs was recorded at 50 $\mu g.mL^{-1}$ against MCF-7 cells. In the present study apoptotic potential of synthesized MgONPs was confirmed by morphological evaluation of the MCF-7 treated cells by AO and EB staining. Apoptosis can be detected by many parameters like the activation of caspase, DNA fragmentation, or changes to cell morphology (Elmore, 2007).

4. Conclusion

The study highlighted the capacity of MgONPs as an antibiofilm against uropathogens and potential cytotoxicity against MCF-7 cells. The results clearly revealed a significant reduction of the biofilm formation upon treatment of MgONPs, and the wide spectrum of morphological differences in biofilm architectures. We believe that the present study will encourage further studies on the applications of MgONPs as potential biocompatible and nanomaterial for *in vitro* and *in vivo* application. Further *in vitro* and *in vivo* studies are required to support our observations of the antibiofilm and anti-tumor potential of these MgONPs.

Acknowledgment

The authors gratefully acknowledge the financial support from the DBT (Govt. of India), for the establishment of National Repository for Microalgae and Cyanobacteria – Freshwater (BT/PR7005/PBD26/357/2012). This study was supported by the National Research Foundation of Korea (NRF) funded by the Korean Government (No 2016R1D1A1A09918072).

Appendix A. Supplementary data

Supplementary data to this article can be found online at https://doi.org/10.1016/j.bcab.2019.101069.

References

Albrecht, G., Bernstein, R., Cahn, W.L., Freedman, J.C., Hewitt, C., 2006. Report of the dark energy task force. Astrophysics, 0609591. https://arxiv.org/abs/astro-ph/0609591.

Barr-Beare, E., Saxena, V., Hilt, E.E., Thomas-White, K., Schober, M., Schwaderer, A.L., 2015. The interaction between Enterobacteriaceae and calcium oxalate deposits. PLoS One 10, e0139575.

Boca, S.C., Potara, M., Gabudean, A.M., Juhem, A., Baldeck, P.L., Astilean, S., 2011. Chitosan-coated triangular silver nanoparticles as a novel class of biocompatible, highly effective photothermal transducers for in vitro cancer cell therapy. Cancer Lett. 311 (2), 131–140.

Buchanan, R.E., Gibbons, N.E., 1974. Bergey's Manual of Deteminative Bacteriology. The Williams & Wilkins Company.

Cai, L., Chen, J., Liu, Z., Wang, H., Yang, H., Ding, W., 2018. Magnesium oxide nanoparticles: effective agricultural antibacterial agent against Ralstonia solanacearum. Front. Microbiol. 9.

Chandra, H.J., Rao, B.S., Manzoor, M.A.P., Arun, A.B., 2017. Characterization and antibiotic sensitivity profile of bacteria in orofacial abscesses of odontogenic origin. J Maxillofac Oral Surg 16 (4), 445–452.

Chari, N., LewisOscar, F., Davoodbasha, M., Ali, A.S., Nooruddin, T., 2017. *In vitro* and *in vivo* antibiofilm effect of copper nanoparticles against aquaculture pathogens. Biocatal. Agric. Biotechnol. 10, 336–341.

Darzynkiewicz, Z., Li, X., 1994. Gong Assays of cell viability: discrimination of cells dying by apoptosis. Methods Cell Biol. 41, 15–38.

Donlan, R.M., 2001. Biofilms and device-associated infections. Emerg. Infect. Dis. 7 (2), 277–281.

Elmore, S., 2007. Apoptosis: a review of programmed cell death. Toxicol. Pathol. 35 (4), 495–516.

Ghosh, K., Ray, M., Adak, A., Halder, A.K., Das, A., Jana, A., Mondal, K.C., 2015. Role of probiotic *Lactobacillus fermentum* KKL1 in the preparation of a rice based fermented beverage. Bioresour. Technol. 188, 161–168.

Gopinath, V., MubarakAli, D., Priyadarshini, S., MeeraPriyadarshini, N., Thajuddin, N., Velusamy, P., 2012. Biosynthesis of silver nanoparticles from *Tribulus terrestris* and its antimicrobial activity: a novel biological approach. Colloids Surfaces B Biointerfaces 96, 69–74.

Gopinath, V., Priyadarshini, S., Saravanan, M., MubarakAli, D., 2015. *Tribulus terrestris* leaf mediated biosynthesis of stable antibacterial silver nanoparticles. Pharm. Nanotechnol. 3 (1), 26–34.

Hayat, T., Khan, M.I., Imtiaz, M., Alsaedi, A., 2018. Heat and mass transfer analysis in the stagnation region of Maxwell fluid with chemical reaction over a stretched surface. J. Therm. Sci. Eng. Appl. 10 (1), 011002–011008.

Huang, L., Li, D.Q., Lin, J., Wei, M., Evans, D.G., Duan, X., 2005. Controllable preparation of Nano-MgO and investigation of its bactericidal properties. J. Inorg. Biochem. 99 (5), 986–993.

Huh, D., Hamilton, G.A., Ingber, D.E., 2011. From 3D cell culture to organs-on-chips. Trends Cell Biol. 21 (12), 745–754.

Jemal, A., Siegel, R., Xu, J., Ward, J.E., 2010. Cancer statistics. CA Cancer J. Clin. 60 (5), 277–300.

Jeyaraj, M., Sathishkumar, G., Sivanandhan, G., MubarakAli, D., Rajesh, M., Arun, R., Kapildev, G., Manickavasagam, M., Sivaramakishnan, S., Thajuddin, N., Premkumar, K., Ganapathi, A., 2013. Biogenic silver nanoparticles for cancer treatment: an experimental report. Colloids Surfaces B Biointerfaces 106, 86–92.

Khan, D.M., Manzoor, M.A.P., Rao, I.V., Moosabba, M.S., 2019. Evaluation of biofilm formation, cell surface hydrophobicity and gelatinase activity in Acinetobacter baumannii strains isolated from patients of diabetic and non-diabetic foot ulcer infections. Biocatal Agric Biotechnol 18, 101007. https://doi.org/10.1016/j.bcab.2019.01.045.

Koo, H., Allan, R.N., Howlin, R.P., Stoodley, P., Hall-Stoodley, L., 2017. Targeting microbial biofilms: current and prospective therapeutic strategies. Nat. Rev. Microbiol. 15 (12), 740–755.

Lee, A.V., Oesterreich, S., Davidson, N.E., 2015. MCF-7 cells, Changing the course of breast cancer research and care for 45 years. J. Natl. Cancer Inst. 107 (7), 73–76.

Leung, Y.H., Ng, A., Xu, X., Shen, Z., Gethings, L.A., Wong, M.T., Lee, P.K., 2014. Mechanisms of antibacterial activity of MgO: non-ROS mediated toxicity of MgO nanoparticles towards *Escherichia coli*. Small 10 (6), 1171–1183.

LewisOscar, F., MubarakAli, D., Priyanka, R., Nithya, C., Gopinath, V., Naif Al-Harbi, S., Thajuddin, N., 2015. One pot synthesis and potential antibiofilm property of copper nanoparticles against clinically isolated strains of *Pseudomonas aeruginosa*. Biofouling 31 (4), 379–391.

Limsuwan, S., Voravuthikunchai, S.P., 2008. Boesenbergia pandurata (Roxb) Schltr, *Eleutherine americana Merr* and *Rhodomyrtus tomentosa* (Aiton) Hassk as antibiofilm producing and antiquorum sensing in *Streptococcus pyogenes*. Immunol. Med. Microbiol. 53 (3), 429–436 2008.

Manzoor, M.A.P., Mujeeburahiman, M., Rekha, P.D., 2017. Association of serum biochemical panel with mineralogical composition of kidney stone in India. Acta Med. Int. 4 (2), 26–30.

Manzoor, M.A.P., Mujeeburahiman, M., Rekha, P.D., 2018a. Electron probe micro-analysis reveals the complexity of mineral deposition mechanisms in urinary stones. Urolithiasis 46, 1–12.

Manzoor, M.A.P., Duwal, S.R., Mujeeburahiman, M., Rekha, P.D., 2018b. Vitamin C inhibits crystallization of struvite from artificial urine in the presence of *Pseudomonas aeruginosa*. Int. Braz J. Urol. 44 (6), 1234–1242.

Manzoor, M.A.P., Shabeena, K.S., Mujeeburahiman, M., Khan, A., 2018c. In dwelling J ureteral stents associated asymptomatic bacteraemia caused by multidrug resistant strain of *Kocuria kristinae*. J. Clin. Diagn. Res. 12 (5), 15–16.

Manzoor, M.A.P., Singh, B., Agrawal, A.K., Arun, A.B., Mujeeburahiman, M., Rekha, P.D., 2018d. Morphological and micro-tomographic study on evolution of struvite in synthetic urine infected with bacteria and investigation of its pathological biomineralization. PLoS One 13 (8), e0202306.

Manzoor, M.A.P., Mujeeburahiman, M., Duwal, S.R., Rekha, P.D., 2019. Investigation on growth and morphology of *in vitro* generated struvite crystals. Biocatal Agric Biotechnol 17, 566–570.

Markowska, K., Grudniak, A.M., Wolska, K.I., 2013. Silver nanoparticles as an alternative strategy against bacterial biofilms. Acta. Biochim. 60, 523–530.

Mosmann, T., 1983. Rapid colorimetric assay for cellular growth and survival: application

to proliferation and cytotoxicity assays. J. Immunol. Methods 65 (1–2), 55–63.
MubarakAli, D., Arunkumar, J., Nag, K.H., SheikSyedIshack, K.A., Baldev, E., Pandiaraj, D., Thajuddin, N., 2013a. Gold nanoparticles from Pro and eukaryotic photosynthetic microorganisms Comparative studies on synthesis and its application on biolabelling. Colloids Surfaces B Biointerfaces 103, 166–173.
MubarakAli, D., Arunkumar, J., Pooja, P., Subramanian, G., Thajuddin, N., Harbi, N., 2015a. Synthesis and characterization of biocompatible tenorite nanoparticles for implant coatings with potential property against biofilm formation. Saudi Pharmaceut. J. 23 (4), 421–428.
MubarakAli, D., Arunkumar, J., Rahuman Sheriff, M., Pandiaraj, D., Thajuddin, N., 2013b. Fabrication of silver nanoparticles with cotton for antibacterial wound dressing. Pharm. Nanotechnol. 1 (1), 78–82.
MubarakAli, D., Bo-Ram, Park, Won-Jong, Rhee, Sang-Yul, L., Jung-Wan, K., 2018. Antioxidant potentials of nanoceria synthesized by solution plasma process and its biocompatibility study. Arch. Biochem. Biophys. 645, 42–49.
MubarakAli, D., Sang-Yul, L., Seong-Cheol, K., Jung-Wan, K., 2015b. One-step synthesis and characterization of broad spectrum antimicrobial efficacy of cellulose/silver nanobiocomposites using solution plasma process. RSC Adv. 5, 35052–35060.
MubarakAli, D., Sasikala, D., Gunasekaran, M., Thajuddin, N., 2011a. Biosynthesis and characterization of silver nanoparticles using marine cyanobacterium, *Oscillatoria willei* NTDM01. Digest J. Nanomater. Biostruct. 6, 385–390.
MubarakAli, D., Thajuddin, N., Jeganathan, K., Gunasekaran, M., 2011b. Plant extract mediated synthesis of silver and gold nanoparticles and its antibacterial activity against clinically isolated pathogens. Colloids Surfaces B Biointerfaces 85, 360–365.
MubarakAli, D., Divya, C., Gunasekaran, M., Thajuddin, N., 2011c. Biosynthesis and characterization of Silicon-Germanium oxide nanocomposite by Diatom. Digest J. Nanomater. Biostruct. 6, 117–120.
Naiyf, S., Jamal, M., 2017. Growth inhibition and antibiofilm potential of Ag nanoparticles coated with lectin, an invertebrate immune molecule. J. Photochem. Photobiol., A 1, 208–216.
Park, H.J., Kim, H.Y., Cha, S., Ahn, C.H., Roh, J., Park, S., Yoon, J., 2013. Removal characteristics of engineered nanoparticles by activated sludge. Chemosphere 92 (5), 524–528.
Priyadarshini, S., Gopinath, V., Priyadharsshini, N.M., MubarakAli, D., Velusamy, P., 2013. Synthesis of anisotropic silver nanoparticles using novel strain, *Bacillus flexus* and its biomedical application. Colloids Surfaces B Biointerfaces 102, 232–237.
Shabeena, K.S., Bhargava, R., Manzoor, M.A.P., Mujeeburahiman, M., 2018. Characteristics of bacterial colonization after indwelling double-J ureteral stents for different time duration. Urol. Ann. 10 (1), 71–75.
Vahedi, N., Hosseini-Jazani, S., Yousefi, M., Ghahremani, M., 2017. Evaluation of antibacterial effects of nickel nanoparticles on biofilm production by *Staphylococcus epidermidis*, Iran. J. Microbiol. 9 (3), 160–168.
Zhang, K., An, Y., Zhang, L., Dong, Q., 2012. Preparation of controlled nano-MgO and investigation of its bactericidal properties. Chemosphere 89 (11), 1414–1418.